The LHCf experiment at the Large Hadron Collider: status and prospects

Alessio Tiberio[a,b,*] **for the LHCf collaboration**

[a]*University of Firenze, Department of Physics and Astronomy*
Via Sansone 1, Sesto Fiorentino, Firenze, Italy

[b]*INFN Section of Firenze,*
Via Sansone 1, Sesto Fiorentino, Firenze, Italy

E-mail: alessio.tiberio@fi.infn.it

The LHC-forward experiment (LHCf), located at the Large Hadron Collider (LHC), is designed to measure the production cross section of neutral particles in the pseudorapidity region above 8.4, up to zero-degree. The measurement of the very-forward particle production rates at the highest energy available at an accelerator will provides fundamental informations for the tuning of the phenomenological hadronic interaction models used in the simulation of air-showers induced by ultra-high-energy cosmic rays in the Earth atmosphere. The experiment consists of two small independent detectors placed 140 metres away from the ATLAS interaction point (IP1), on opposite sides. Each detector is made of two sampling and position sensitive calorimeters. This contribution will firstly highlight the Run II physics results of LHCf in proton-proton collisions at 13 TeV: the photon and neutron production spectra will be presented and compared with the predictions of several hadronic interaction models commonly used in air-shower simulations. Furthermore, the advantages of the ATLAS-LHCf combined analysis will be discussed and the energy spectrum of very-forward photons produced in diffractive collisions (tagged by ATLAS central detectors) will be shown together with models predictions. Later, a report of the successful LHCf data taking during its dedicated run with proton-proton collisions at 13.6 TeV performed on September 2022 will be presented. Finally, the physics motivation of the foreseen operation with proton-oxygen collisions at the LHC will be illustrated.

*Speaker

PoS(ICRC2023)444

1. Introduction

The study of the the Ultra-High-Energy Cosmic Rays (UHECRs), with energies $\gtrsim 10^{18}$ eV, is only possible using indirect observation techniques. The detection of UHECRs is performed through the observation of the shower of secondary particles produced in the interaction of the UHECR with a nucleus of the atmosphere (the so-called "air-showers"). The interpretation of the data of ground based experiments relies on a detailed simulation of the air-showers in order to reconstruct the astrophysical parameters of the primary cosmic ray from the observables measured from the secondary particles. Due to the large systematic uncertainty associated to the disagreement between different hadronic interaction models employed in the simulations of the air-showers, a tuning of these phenomenological models with experimental data is fundamental to improve the precision of UHECR measurements.

The LHC-forward experiment (LHCf) [1] is designed to measure the very-forward neutral particles production at the Large Hadron Collider (LHC) [2]. The very-forward region covered by LHCf is crucial for the tuning of hadronic interaction models since it is the region where most of the energy flow of secondary particles is contained. A description of the LHCf experimental apparatus is given in Section 2. The LHCf analysis results for photon and neutron production in proton-proton collisions at $\sqrt{s}$ = 13 TeV will be presented in Section 3. A summary of the LHCf operation with proton-proton collisions at $\sqrt{s}$ = 13.6 TeV will be given in Section 4, while the motivation of the foreseen p-O run is explained in Section 5.

2. The LHCf experiment

The LHCf experiment is composed of two independent detectors (named "Arm1" and "Arm2") placed ~140 meters away from the Interaction Point 1 [1]. The detectors are placed in the Target Absorber Neutral (TAN) instrumentation slot, where the beam pipe from the interaction point turns into two separate beam pipes: the detectors are then able to measure neutral particles emitted at a pseudorapidity $\gtrsim 8.4$, up to zero-degree, while charged particles are deflected by the dipole magnets which bend the colliding beams into their own beam pipes.

Each detector is made of two sampling and position sensitive calorimeters (called "towers" hereafter) which use Gd_2SiO_5 (GSO) scintillators as active layers and tungsten as absorber. The differences between Arm1 and Arm2 are the transverse size of the towers and the detectors used for the measurement of the transverse coordinate: Arm1 employs arrays of GSO scintillator bars, while Arm2 uses silicon microstrip detectors. Each tower has a depth of 44 radiation lengths and 1.6 hadronic interaction lengths. The energy resolution is better than 3% for photons above 100 GeV [3] and ~40% for neutrons. The position resolution for photons is 200 μm and 40 μm for Arm1 and Arm2 [3, 4], respectively, while the position resolution for neutrons is ~1 mm for both detectors.

3. LHCf physics results in p-p collisions at $\sqrt{s}$ = 13 TeV

The photon and neutron analyses were performed on a dataset of 0.19 nb^{-1} collected during the low-luminosity LHCf dedicated run in proton-proton collisions at $\sqrt{s}$ = 13 TeV in LHC fill #3855.

A dedicated low-luminosity beam setup was used with a luminosity of $0.4 \div 1.4 \times 10^{29}$ cm^{-2} s^{-1}, $\beta^* = 19$ m and mean number of inelastic collisions per bunch crossing $\mu = {\sim}0.01$. The π^0 and η X_F-P_T spectra are presented in a separate contribution [5].

3.1 Neutron energy spectrum and average inelasticity

The neutron energy spectrum in several pseudorapidity regions is shown in Figure 1 [6]. As noted in a previous analysis [7], LHCf data exhibits a peak structure in the zero-degree region ($\eta > 10.75$) which is not reproduced by any model and all models underestimate the neutron yield by at least 20%. In the other pseudorapidity regions either SIBYLL or EPOS models have a better agreement with respect to other models. From the measured spectra it is also possible to extract the distribution of the elasticity of the collision ($k_n \equiv 2E_n/\sqrt{s}$, where E_n is the energy of the neutron). The k_n distribution is shown in the left panel of Figure 2. The average inelasticity ($\langle 1 - k_n \rangle$) is shown in the right panel of the same figure. While the average inelasticity predicted by all models is in good agreement with the measured one, the k_n distribution varies significantly between models and no one is in good agreement with data.
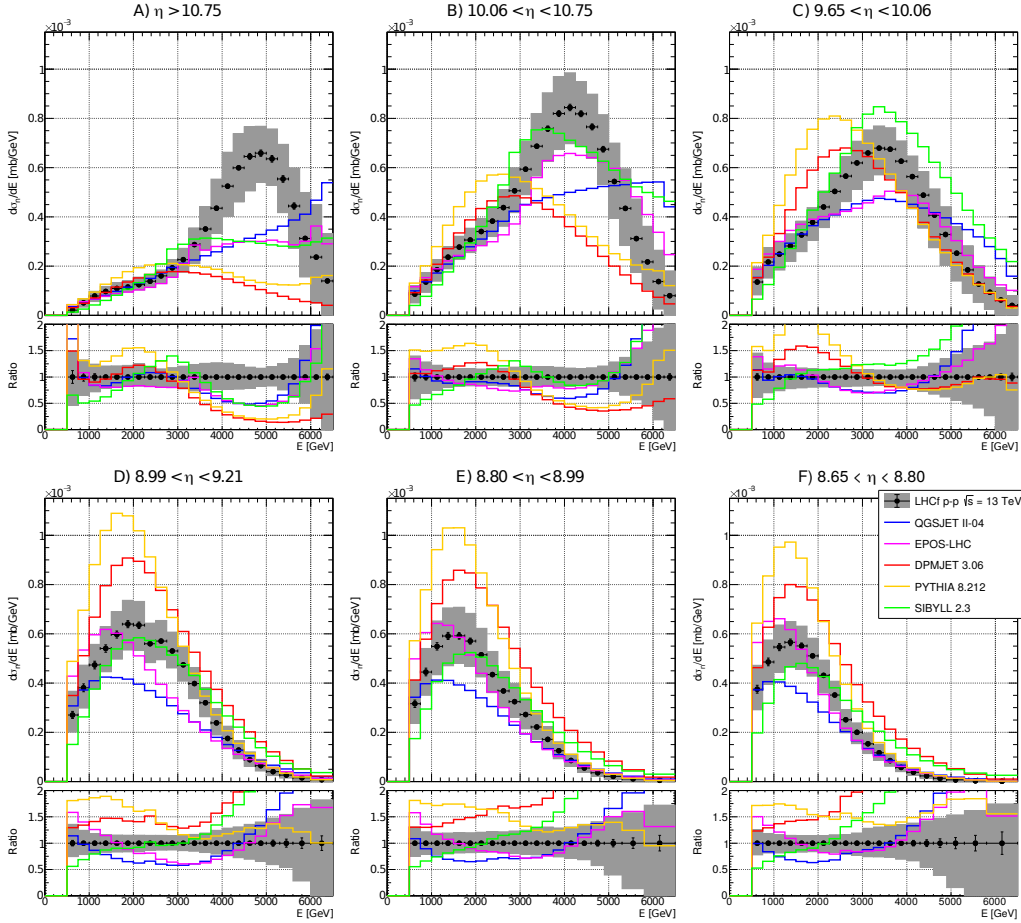

Figure 1: Measured neutron energy spectrum (black points) in different pesudorapidity bins compared with models predictions (coloured histograms). Grey area represents statistical+systematic uncertainty [6].
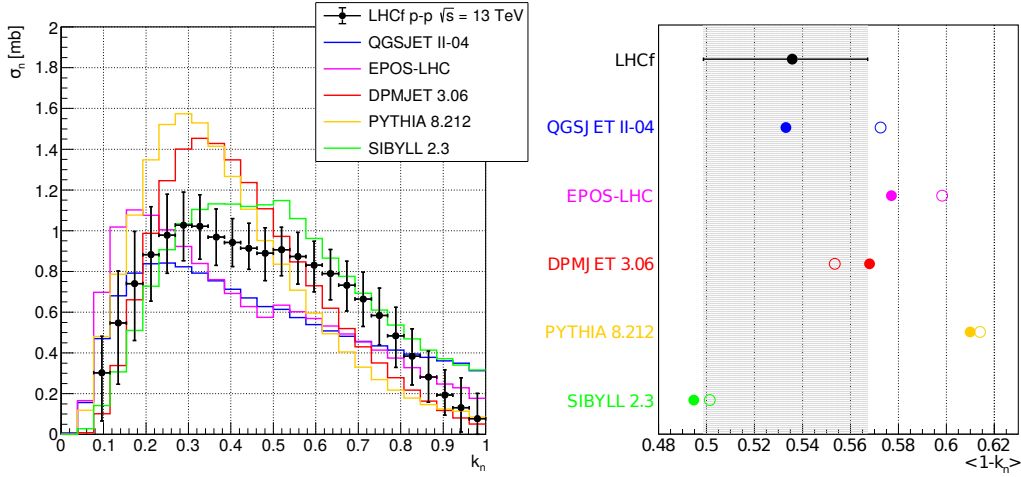
Figure 2: Left: neutron elasticity distribution for data (black points) and models predictions (coloured histograms). Right: average inelasticity for neutron events (full circles) and all event (open circles) [6].

3.2 LHCf-ATLAS combined photon analysis

The LHCf experiment alone does not have the capability to identify which process happened during the collision occurred at the interaction point. LHCf and ATLAS experiments had a trigger exchange during all LHCf dedicated runs of Run II in order to have the possibility to perform a combined analysis. The first analysis performed is the study of the photon spectrum of diffractive events [8]. The number of tracks recorded by ATLAS detectors in the central region has been used to discriminate diffractive events from non-diffractive ones by requiring no charged particles in the region $|\eta| < 2.5$ [9]. A pure sample of low-mass ($M_X < 20$ GeV) diffraction events has been selected in this way. The preliminary results of the combined analysis are presented in Figure 3 , where the photon energy spectrum is shown for both the inclusive [10] and the low-mass diffraction component [8]. The diffraction spectrum of EPOS model has a good agreement with data in the $\eta > 10.94$ region, while PYTHIA model has a better agreement for $8.81 < \eta < 8.99$. This analysis has been completed and the results are going to be published in a forthcoming publication.

The currently ongoing analysis is the study of the mechanism of multiparton interaction using neutron events in LHCf, as proposed by [11]. This study is performed by measuring the distribution of the number of charged tracks detected by ATLAS in the central region as a function of the energy of the neutron detected by LHCf. This measurement is very important since it can discriminate between hadronic interaction models with a strong central-forward correlation (like QGSJET and EPOS) with respect to the ones with a weaker correlation (like SIBYLL and PYTHIA). The predictions of several hadronic interaction models are shown in Figure 4.

4. LHCf run with p-p collisions at 13.6 TeV

The physics motivations of the LHCf p-p run at 13.6 TeV can in 2022 be summarized as follow:

1. π^0, η and K_S^0 mesons production. Thanks to the expected much higher statistics with respect to Run II, a much more precise measurement of π^0 X_F-P_T spectrum will be possible. The
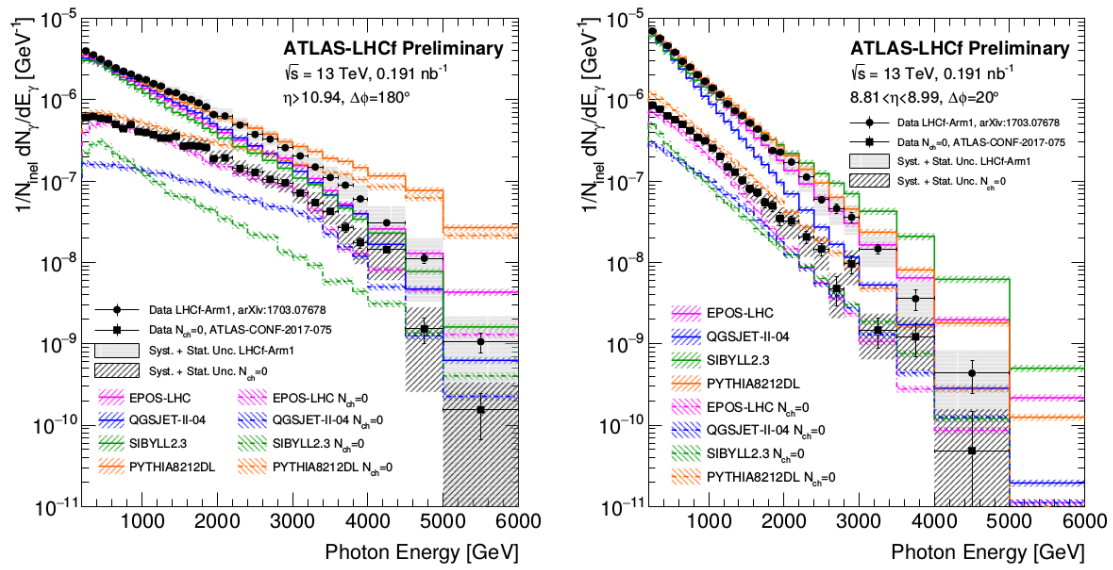
Figure 3: Photon energy spectrum for pseudorapidity regions $\eta > 10.94$ (left) and $8.81 < \eta < 8.99$ (right). Measured inclusive and low-mass diffractive spectra are represented as black circles and squares, respectively. Predictions from several hadronic interaction models for the inclusive and diffractive spectra are represented as solid and dashed lines, respectively. Hatched areas show total error for data and statistical error for models [8].
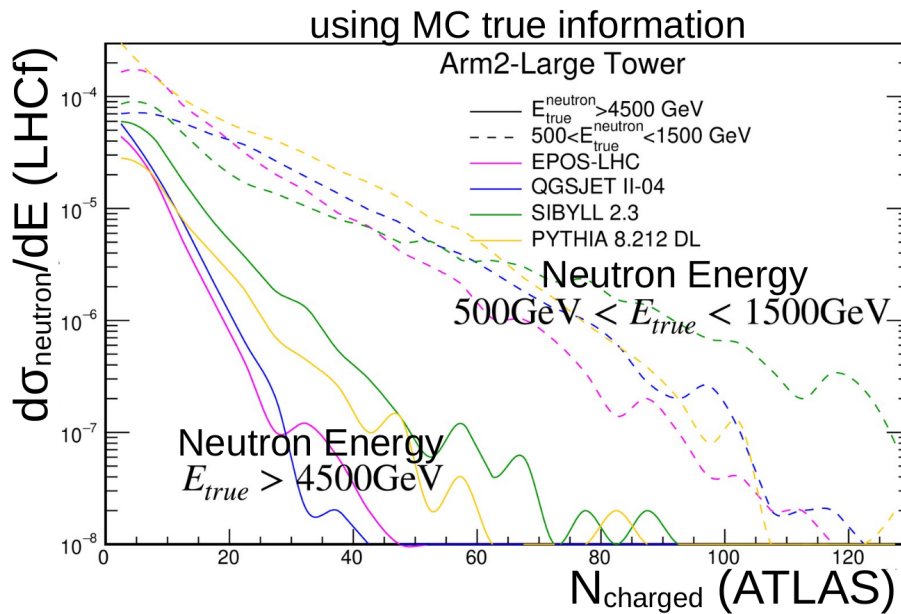

Figure 4: Predictions of several hadronic interaction models on the distribution of the number of charged particles in the central ATLAS detectors in two different energy ranges of neutrons detected by LHCf.

5

measurement of P_T dependence of η X_F spectrum (previously measured in a single P_T bin due to the limited statistics) will also be possible. Finally, a few hundreds of K_S^0 events are expected to be observed.

2. Study of one pion exchange process. The cross section and secondary particles production of a high energy pion-proton collision can be studied measuring the pion exchange process in proton-proton collisions [12]. Thank to the common data taking with ATLAS ZDC, done for the first time in this operation, it is possible to improve the energy resolution of the neutron produced in the pion exchange process measured by LHCf from 40% to 20% [13]. The informations from the central ATLAS detectors can be used to reject the background from other processes.

3. Δ^+ resonance. The detection of a π^0 and a proton on the same side can lead to a measurement of the Δ^+ baryon production in the forward region. This can be achieved by the common data taking of LHCf and ATLAS roman pots, where the former detects a π^0 and the latter detect a proton.

4. Diffractive dissociation. By the measurement of a scattered proton in ATLAS roman pots and particle production in LHCf on the other side it is possible to study the single diffraction dissociation process. The simultaneous detection of the proton and of the diffraction products gives the possibility to both measure the diffractive mass and the particle production.

Before the data taking, an upgrade of the Arm2 silicon readout electronics was performed. The old electronics based on 100 Mbit/s Fiber Optical Transmitter/Receiver Interface (FOXI) transmitters were replaced with a new configuration based on Gbit/s fast optical links. Thanks to this upgrade the Arm2 DAQ speed is no longer limited by the silicon electronics and the DAQ speed was increased from 0.5 to 1.5 kHz.

The LHCf operation with proton-proton collisions at $\sqrt{s}$ = 13.6 TeV was performed from the 23th to the 26th of September 2022. A dedicated low-luminosity run was set up with β^* = 19 m and a mean number of inelastic collisions per bunch crossing μ = 0.04. LHCf took data during fills 8178 and 8179, with a duration of 55 (the longest fill ever made in LHC) and 2 hours, respectively. Data were acquired in two different positions: the first position with the small tower placed on the beam center and the second with the detector shifted up by 5 mm in order to extend the pseudorapidity coverage. An integrated luminosity of 40 nb^{-1} were acquired for each detector position, a ~8 times larger statistics with respect to the proton-proton operation in Run II. A schematic view of LHCf position with respect to ATLAS detectors involved in the common data taking is shown in Figure 5. A preliminary distribution of the di-photon invariant mass measured by LHCf in Run III is shown in Figure 6, where the π^0 and η peaks are clearly visible.

5. The proton-Oxygen run in 2024

A LHC run with proton-oxygen collisions is foreseen during 2024. The p-O collision case is the best configuration to study the interaction of a cosmic ray (mainly a light nucleus) with a nucleus of the atmosphere (mainly nitrogen or oxygen). A direct measurement of the p-O interaction cross section and particle production will avoid the need to perform large extrapolations from p-p results.
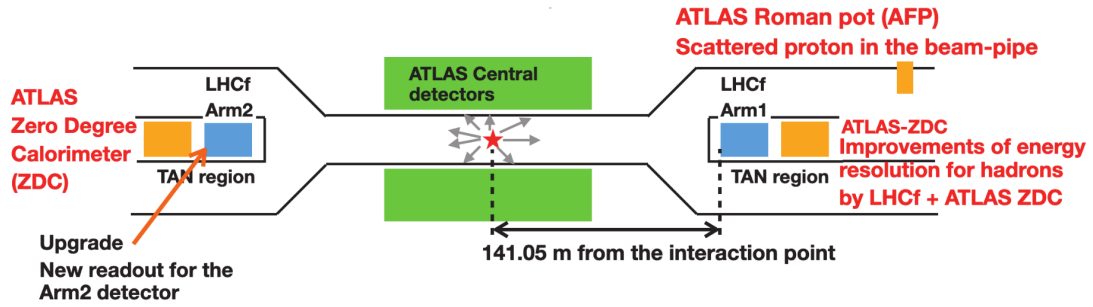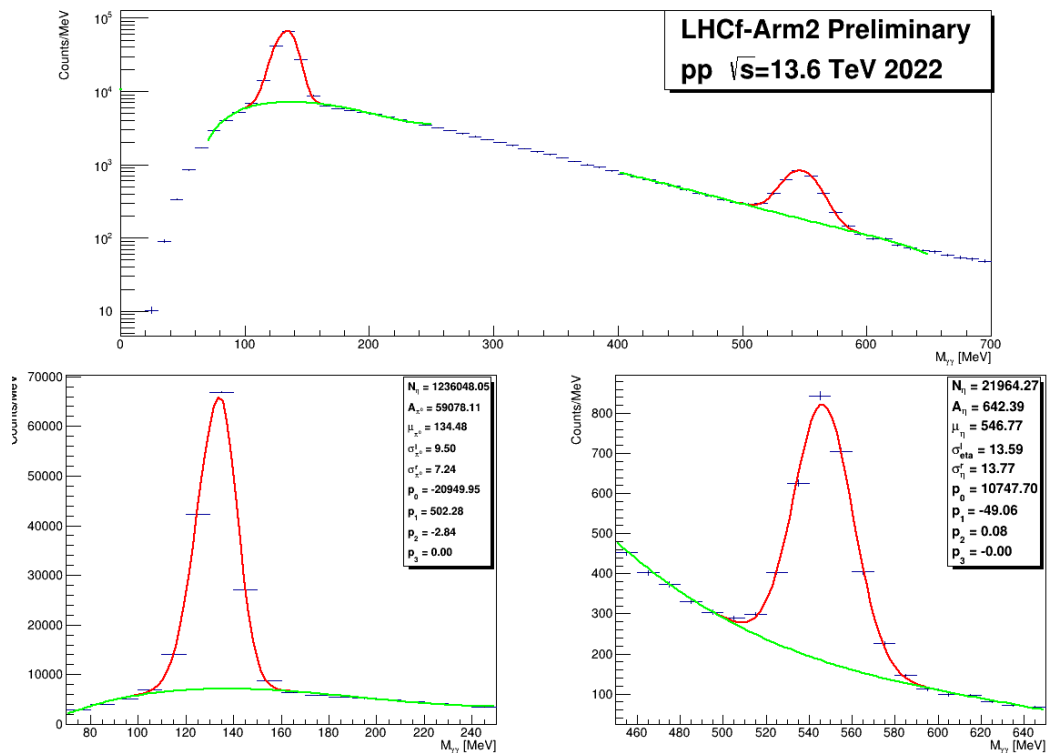
Figure 5

Figure 6: Invariant mass distribution of pair of photons (detected in different towers) with proton-proton collisions at $\sqrt{s}$ = 13.6 TeV. The result of the composite fit with an asymmetric gaussian and a polynomial background for each peak is also shown.

Another advantage of p-O collisions is that the contribution from ultra peripheral collisions (UPC) in the particle production is negligible with respect to QCD one. Since UPCs are not relevant for air shower simulations, in order to provide results that can be used for the tuning of hadronic interaction models the UPC contribution must be estimated with a MC simulation and subtracted from data: the uncertainty on the UPC simulation add a significant contribution to the systematic uncertainty of the measurement. This happens in p-Pb measurements where the UPC contribution

is of the same order of QCD one.

LHCf is able to operate on the p-remnant side where the multiplicity of particles in a single tower is still manageable. On the O-remnant side LHCf can still operate but with the detector shifted up by at least 15 mm in order to have a reasonable multiplicity in the detector.

References

[1] O. Adriani et al., *The LHCf detector at the CERN large hadron collider*, *Journal of Instrumentation* **3** (2008) S08006.

[2] L. Evans, *The Large Hadron Collider*, *New Journal of Physics* **9** (2007) 335.

[3] Y. Makino et al., *Performance study for the photon measurements of the upgraded LHCf calorimeters with Gd_2SiO_5 (GSO) scintillators*, *Journal of Instrumentation* **12** (2017) P03023.

[4] O. Adriani et al., *The construction and testing of the silicon position sensitive modules for the LHCf experiment at CERN*, *Journal of Instrumentation* **5** (2010) P01012.

[5] G. Piparo et al., *Measurement of the very forward π^0 and eta meson productions in p-p collisions at $\sqrt{s}$=13 TeV with the LHCf detector*, *PoS* (ICRC2023) 447.

[6] O. Adriani et al., *Measurement of energy flow, cross section and average inelasticity of forward neutrons produced in $\sqrt{s}$ = 13 TeV proton-proton collisions with the LHCf Arm2 detector*, *Journal of High Energy Physics* **2020** (2020) 16.

[7] O. Adriani et al., *Measurement of inclusive forward neutron production cross section in proton-proton collisions at $\sqrt{s}$ = 13 TeV with the LHCf Arm2 detector*, *Journal of High Energy Physics* **2018** (2018) 73.

[8] ATLAS and LHCf Collaborations, *Measurement of contributions of diffractive processes to forward photon spectra in pp collisions at $\sqrt{s}$ = 13 TeV*, *ATLAS-CONF-2017-075* (2017) .

[9] Q.-D. Zhou, Y. Itow, H. Menjo and T. Sako, *Monte Carlo study of particle production in diffractive proton–proton collisions at $\sqrt{s}$ = 13 TeV with the very forward detector combined with central information*, *The European Physical Journal C* **77** (2017) 212.

[10] O. Adriani et al., *Measurement of forward photon production cross-section in proton–proton collisions at $\sqrt{s}$ = 13 TeV with the LHCf detector*, *Physics Letters B* **780** (2018) 233.

[11] S. Ostapchenko, M. Bleicher, T. Pierog and K. Werner, *Constraining high energy interaction mechanisms by studying forward hadron production at the LHC*, *Phys. Rev. D* **94** (2016) 114026.

[12] V.A. Petrov, R.A. Ryutin and A.E. Sobol, *LHC as πp and $\pi\pi$ collider*, *The European Physical Journal C* **65** (2010) 637.

[13] M. Kondo et al., *Performance evaluation of LHCf-ATLAS ZDC joint measurement using proton beam*, *EPJ Web Conf.* **283** (2023) 05012.

Full Authors List: LHCf Collaboration

O. Adriani[1,2], E. Berti[2], P. Betti[1,2] L. Bonechi[2], M. Bongi[1,2], R. D'Alessandro[1,2], M. Haguenauer[3], Y. Itow[4,5], K. Kasahara[6], M. Kondo[4], Y. Matsubara[4], H. Menjo[4], Y. Muraki[4], K. Ohashi[4], P. Papini[2], G. Piparo[7,8] S. Ricciarini[2,9], T. Sako[10], N. Sakurai[11], M. Scaringella[2], Y. Shimizu[12], T. Tamura[12], A. Tiberio[1,2], S. Torii[13], A. Tricomi[7,8,14], W. C. Turner[15], and K. Yoshida[6]

[1] University of Firenze, Firenze, Italy
[2] INFN Section of Firenze, Firenze, Italy
[3] Ecole-Polytechnique - Palaiseau, France
[e] Institute for Space-Earth Environmental Research, Nagoya University, Nagoya, Japan
[5] Kobayashi-Maskawa Institute for the Origin of Particles and the Universe, Nagoya University, Nagoya, Japan
[6] Faculty of System Engineering, Shibaura Institute of Technology, Japan
[7] University of Catania, Catania, Italy
[8] INFN Section of Catania, Catania, Italy
[9] IFAC-CNR - Florence, Italy
[10] Institute for Cosmic Ray Research, University of Tokyo, Kashiwa, Japan
[11] Tokushima University, Tokushima, Japan
[12] Kanagawa University - Kanagawa, Japan
[13] RISE, Waseda University, Shinjuku, Tokyo, Japan
[14] CSFNSM, Catania, Italy
[15] LBNL, Berkeley, California, USA